Supplemental Fig 1 (related to Figure 1). NLRP14 expression is down-regulated following fertilization, is expressed in certain human cell lines, and is functionally conserved in mouse (a) Expression of NLRP14 mRNA in early preimplantation embryos. Shown is RNA-seq data from Yan et al (2013) (b) NLRP14 expression across 293T, iHBEC, A549, and Caco2 cells (shown are qPCR data relative to GAPDH). (c) Primary human bronchial epithelial cells (HBEC) were challenged with either viral RNA (vRNA) or influenza virus and monitored for IFNβ production (ELISA) or viral replication (NP ELIZA) in the presence or absence of NLRP14 knock-down by siRNA. (d) Knock-down validation of NLRP14 mRNA expression (shown are qPCR data relative to GAPDH). (e) Inhibition of TBK1 mediated activation of IFNβ-, ISRE-, and NFκB-luc reporters by human NLRP14 and mouse nlrp14 in 293T cells. (f) 293T cells were transfected with mouse sting and nlrp14 and monitored for ISRE- and NFκB-luc activity. (g) 293T cells transfected with mouse sting-HA and Myc-nlrp14 were monitored for phospho-TBK1 and phospho-IRF3 by western blot analysis. Data are representative of at least two independent experiments.

Supplemental Fig 2 (related to Figure 3 and Figure 6). Establishment of NLRP14-CRISPR cells in 293T and STING-293T cells. Target sequences and PCR detection of mutated NLRP14 are shown for 293T-NLRP14-CRISPR (a) and 293T-NLRP14-CRISPR cells is shown (genomic DNA was extracted and detection mutations was monitored by PCR and sequencing). (c) Rhodamine-labeled B-DNA (B-DNA Rho) was transfected into parental (WT) and 293-NLRP14-CRISPR (KO) cells and observed by fluorescence microscopy. Data are representative of at least two independent experiments.

Supplemental Fig 3 (related to Figure 4 and 5). NLRP14 regulates signaling following viral infection and interacts with TBK1 . 293T cells were transfected with TBK1-FL (a) or IRF7-FL in combination with Myc-NLRP14 (where indicated) and challenged with NDV-GFP followed by whole cell lysis and monitoring of key signaling events (as indicated) by western blotting. (c) Nuclear translocation of IRF3 was monitored (by western blotting) in 293T and NLRP14-CRISPR cells in response to

NDV-GFP infection. (d) 293T cells were transfected with-Myc NLRP14 and then whole cell lysates were fractionated to determine co-association of NLRP14 with endogenous cellular factors including TBK1. Data are representative of at least two independent experiments.

Supplemental Figure 4. Validation of NLRP14 as the target in NLRP14-CRISPR cells (related to Figure 3). (a) 293T cells were transfected with NLRP14 or NACHT domain of NLRP14 (as indicated) and monitored for the ability to modulate TBK1 mediated activation of IFNβ-, NFκB-, or ISRE-luc activity. Complementation assay to demonstrate the NLRP14 intrinsic affect in NLRP14-CRISPR cells was performed by generating expression plasmids coding for an NLRP14 mutant (NLRP14 Mut) where the gRNA target sequence was mutated such that it could not be targeted for editing (a). Cells were then transfected with indicated constructs and monitored for TBK1 mediated activation of IFNβ-luc (b), phosphorylation of TBK1 and IRF3 (d), or ubiquitination of TBK1 by immunoblotting (e). Data are representative of at least two independent experiments.

Supplemental Figure 5 (related to Figure 2, Figure 6, and Figure 7). NLRP14 function is independent of NLRP4. Genomic DNA (gDNA) was extracted from NLRP4-CRISPR cells sequenced to determine CRISPR editing (a). 293T and 293T-NLRP4-CRISPR cells were stimulated with indicated ligands (25 μg/ml of PolyI:C and NDV-GFP at the m.o.i of 10) and monitored for ISRE-luc activity. 293T-NLRP4-CRISPR cells were cotransfected with TBK1 and NLRP14 and monitored for phosphorylation (c) and ubiquitination (d) of TBK1 by immunoblotting. (e) 293T-NLRP4-CRISPR cells were co-transfected with indicated expression constructs and monitored for activation of IFNβ-luc activation. Data are representative of at least two independent experiments.

Supplemental Figure 6 (related to Figure 5 and Figure 6). NLRP14 LRR negatively regulates NLRP14 dependent induction of TBK1 ubiquitination independently of Lysine 670 on TBK1. (a) 293T cells were cotransfected with MAVS-Flag or STING-HA and NLRP14 or mutants lacking PYD (Δ-PYD), NACHT (Δ-NACHT), or LRR (Δ-LRR) domains. Whole-cell lysates were subjected to immunoblotting using the appropriate antibodies. (b) 293T cells were cotransfected with TBK1 or STING and NLRP14 or Δ-LRR mutant and monitored for IFNβ-luc activation. (d-e) 293T cells were co-transfected with TBK1 or TBK1 containing a K-R mutation at position 670 (a; K670R) and NLRP14 and monitored for reported activation (d) and TBK1 ubiquitination (e) by immunoblotting. (c) Schematic of TBK1 mutant; KD, kinase domain ; ULD, ubiquitin-like domain ; CC, coiled-coil domain. 293T cells were co-transfected with IPS-1-FL and Myc-NLRP14 and treated with DMSO, MG132 (20 μM), or Bafilomycin A1 (100 nM) to monitor affects on NLRP14 degradation. (f) Whole-cell lysates were prepared at indicated time points and subjected to immunoblotting using indicated antibodies. Data are representative of at least two independent experiments.

Supporting Figure 7 (related to Figure 7). Naturally occurring mutation in NLRP14 results in loss of function and recovery of NAS sensing. 293T cells were co-transfected with TBK1-FL and NLRP14-FL or NLRP14 containing one of the SNPs identified (D86V, A375T, D522Q, and M1019I) and monitored for IFNβ- and NFκB-luc activation or subjected to immunoblotting with indicated antibodies. (b) 293T cells were co-transfected with TBK1 and NLRP14 or K108X and mRNA expression of IFNβ and IP10 were determined by real-time PCR. Shown are ΔCT values relative to GAPDH. (c) Schematic of NLRP14 and C-terminal Flag-tagged truncation mutant of NLRP14 (1-108-FL). 293T cells were cotransfected with TBK1 and NLRP14-FL or 1-108-FL (d-f) and monitored for either IFNβ-luc and NFκB-luc promoter or IFNβ and IP10 mRNA expression by real time PCR (e-f). Expression of NLRP14-FL and 1-108-FL was confirmed by immunoblotting (d). Real-time PCR data was normalized to the expression of GAPDH mRNA. Data are representative of at least two independent experiments.

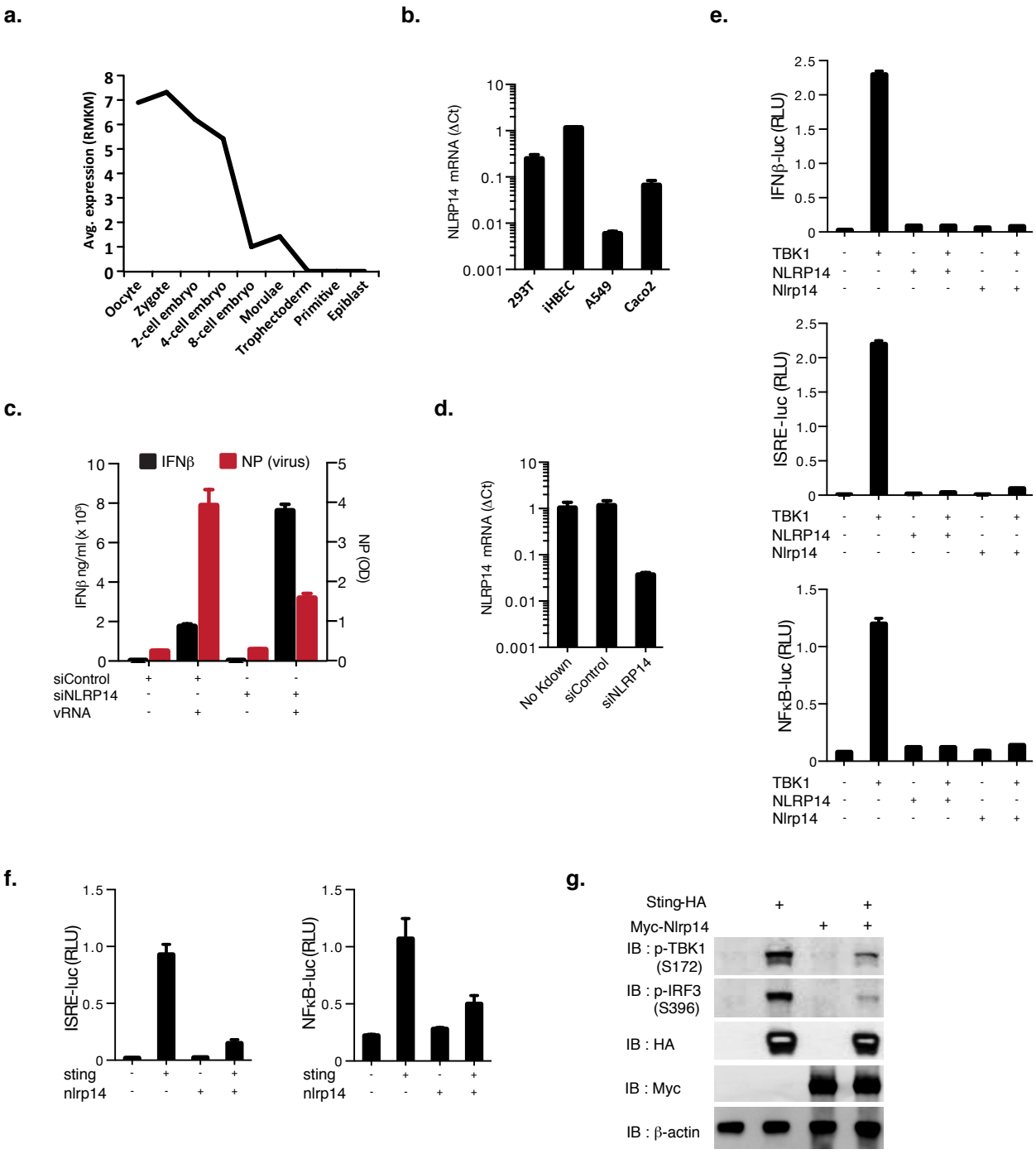
a.
Avg. expression (RMKM)
Oocyte
Zygote
2-cell embryo
4-cell embryo
8-cell embryo
Morulae
Trophectoderm
Primitive
Epiblast
b.
NLRP14 mRNA (ΔCt)
293T
iHBEC
A549
Caco2
e.
IFNβ-luc (RLU)
ISRE-luc (RLU)
NFκB-luc (RLU)
TBK1
NLRP14
Nlrp14
c.
IFNβ
NP (virus)
IFNβ ng/ml (x 10³)
NP (OD)
siControl
siNLRP14
vRNA
d.
NLRP14 mRNA (ΔCt)
No Kdown
siControl
siNLRP14
f.
ISRE-luc (RLU)
NFκB-luc (RLU)
sting
nlrp14
g.
Sting-HA
Myc-Nlrp14
IB : p-TBK1 (S172)
IB : p-IRF3 (S396)
IB : HA
IB : Myc
IB : β-actin

a.

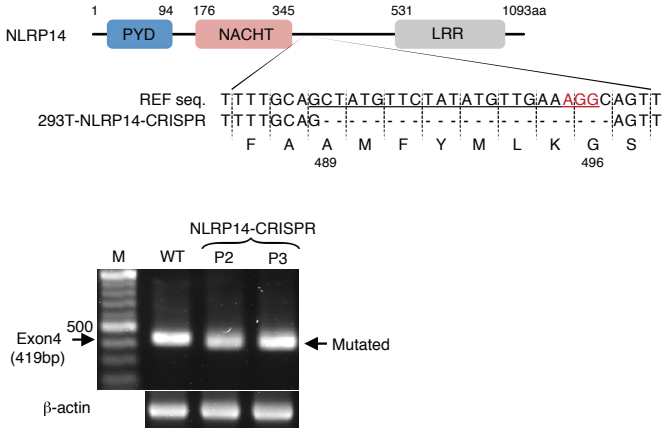
NLRP14
1
94
176
345
531
1093aa
PYD
NACHT
LRR
REF seq. TTTTGCAGCTATGTTCTATATGTTGAAAGGCAGTT
293T-NLRP14-CRISPR TTTTGCAG- - - - - - - - - - - - - - - - - - AGTT
F A A M F Y M L K G S
489
496
NLRP14-CRISPR
M
WT
P2
P3
Exon4
(419bp)
500
Mutated
β-actin

b.

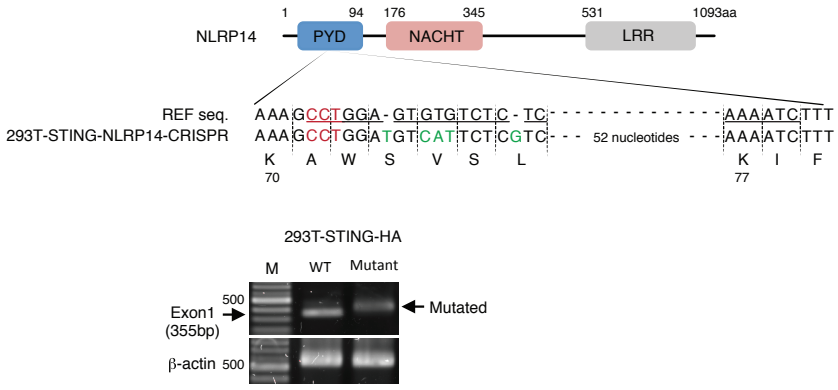
NLRP14
1
94
176
345
531
1093aa
PYD
NACHT
LRR
REF seq. AAAGCCTGGA-GTGTGTCTC-TC- - - - - - - - - - - - - - AAAATCTTT
293T-STING-NLRP14-CRISPR AAAGCCTGGATGTCATTCTCGTC- - - 52 nucleotides - - - AAAATCTTT
K A W S V S L K I F
70
77
293T-STING-HA
M
WT
Mutant
Exon1
(355bp)
500
Mutated
β-actin 500

c.

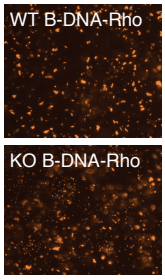
WT B-DNA-Rho
KO B-DNA-Rho

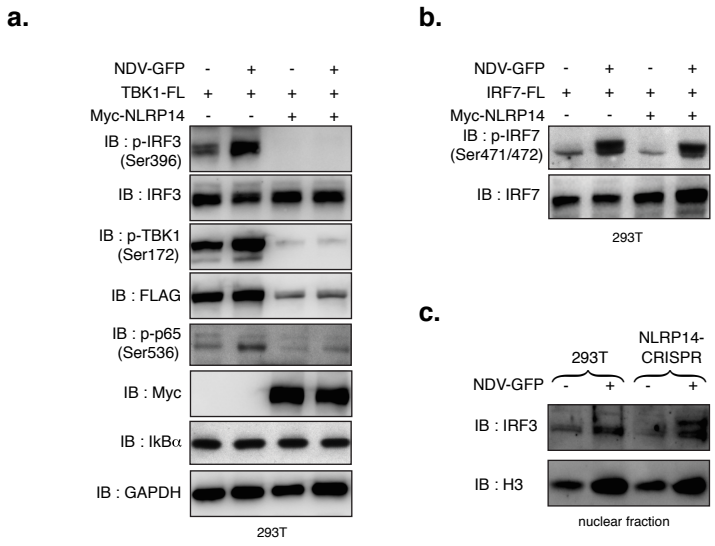
a.
NDV-GFP - + - +
TBK1-FL + + + +
Myc-NLRP14 - - + +
IB : p-IRF3 (Ser396)
IB : IRF3
IB : p-TBK1 (Ser172)
IB : FLAG
IB : p-p65 (Ser536)
IB : Myc
IB : IkBα
IB : GAPDH
293T
b.
NDV-GFP - + - +
IRF7-FL + + + +
Myc-NLRP14 - - + +
IB : p-IRF7 (Ser471/472)
IB : IRF7
293T
c.
293T
NLRP14-CRISPR
NDV-GFP - + - +
IB : IRF3
IB : H3
nuclear fraction

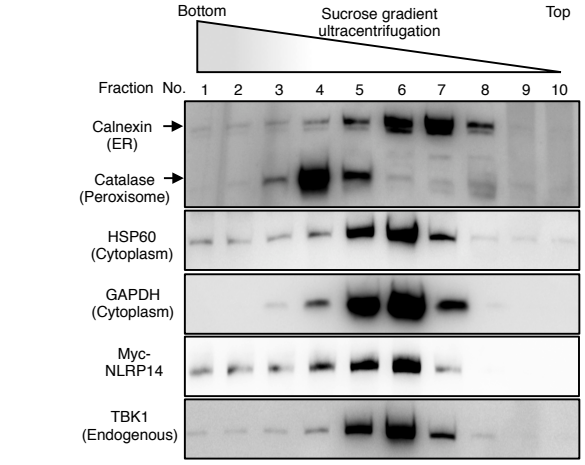
d.
Bottom
Sucrose gradient ultracentrifugation
Top
Fraction No. 1 2 3 4 5 6 7 8 9 10
Calnexin (ER)
Catalase (Peroxisome)
HSP60 (Cytoplasm)
GAPDH (Cytoplasm)
Myc-NLRP14
TBK1 (Endogenous)

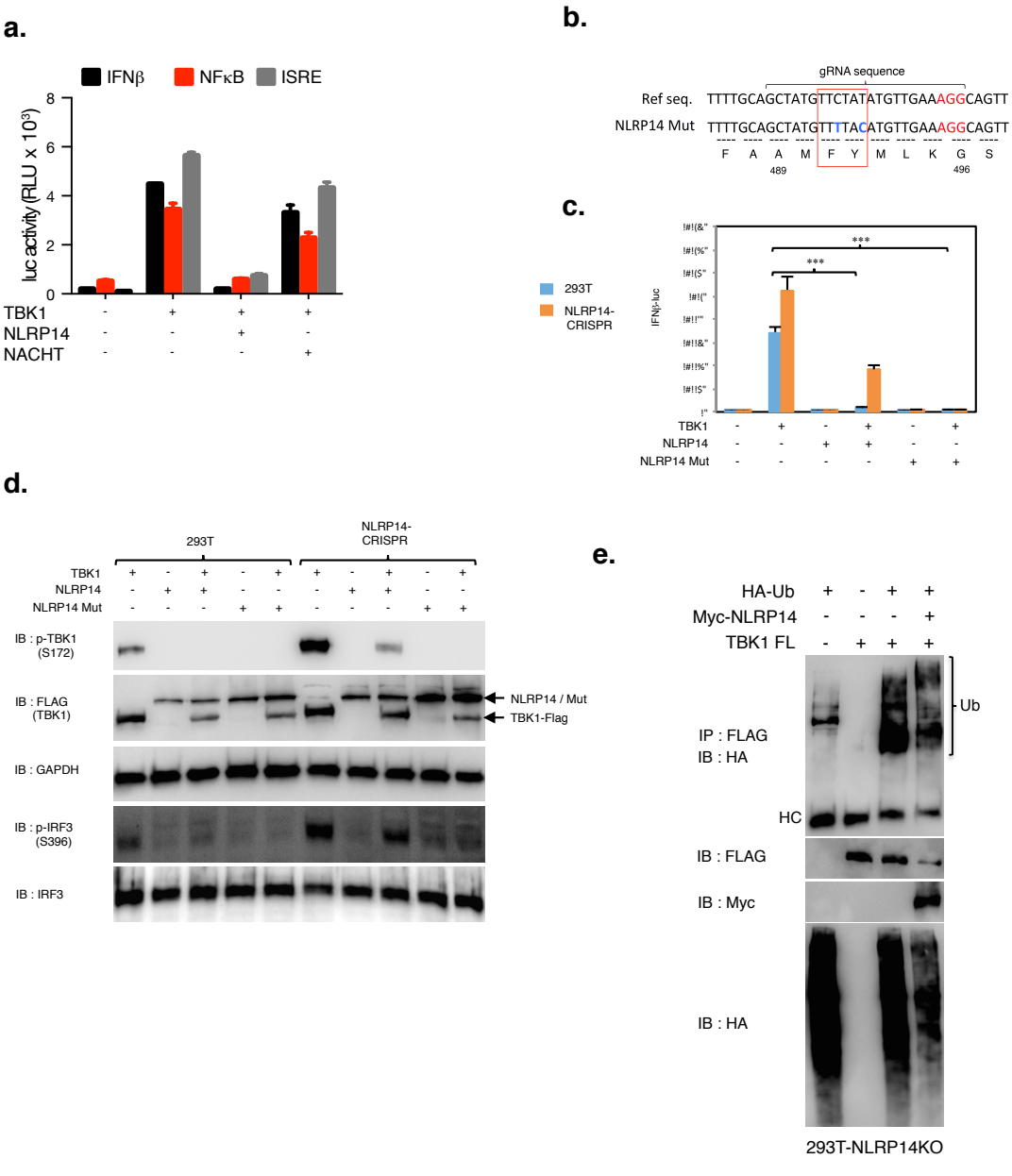
a.
IFNβ
NFκB
ISRE
luc activity (RLU x 10³)
TBK1
NLRP14
NACHT
b.
gRNA sequence
Ref seq. TTTTGCAGCTATGTTCTATATGTTGAAAGGCAGTT
NLRP14 Mut TTTTGCAGCTATGTTTTACATGTTGAAAGGCAGTT
F A A M F Y M L K G S
489
496
c.
293T
NLRP14-CRISPR
IFNβ-luc
TBK1
NLRP14
NLRP14 Mut
d.
293T
NLRP14-CRISPR
TBK1
NLRP14
NLRP14 Mut
IB : p-TBK1 (S172)
IB : FLAG (TBK1)
NLRP14 / Mut
TBK1-Flag
IB : GAPDH
IB : p-IRF3 (S396)
IB : IRF3
e.
HA-Ub
Myc-NLRP14
TBK1 FL
IP : FLAG
IB : HA
Ub
HC
IB : FLAG
IB : Myc
IB : HA
293T-NLRP14KO

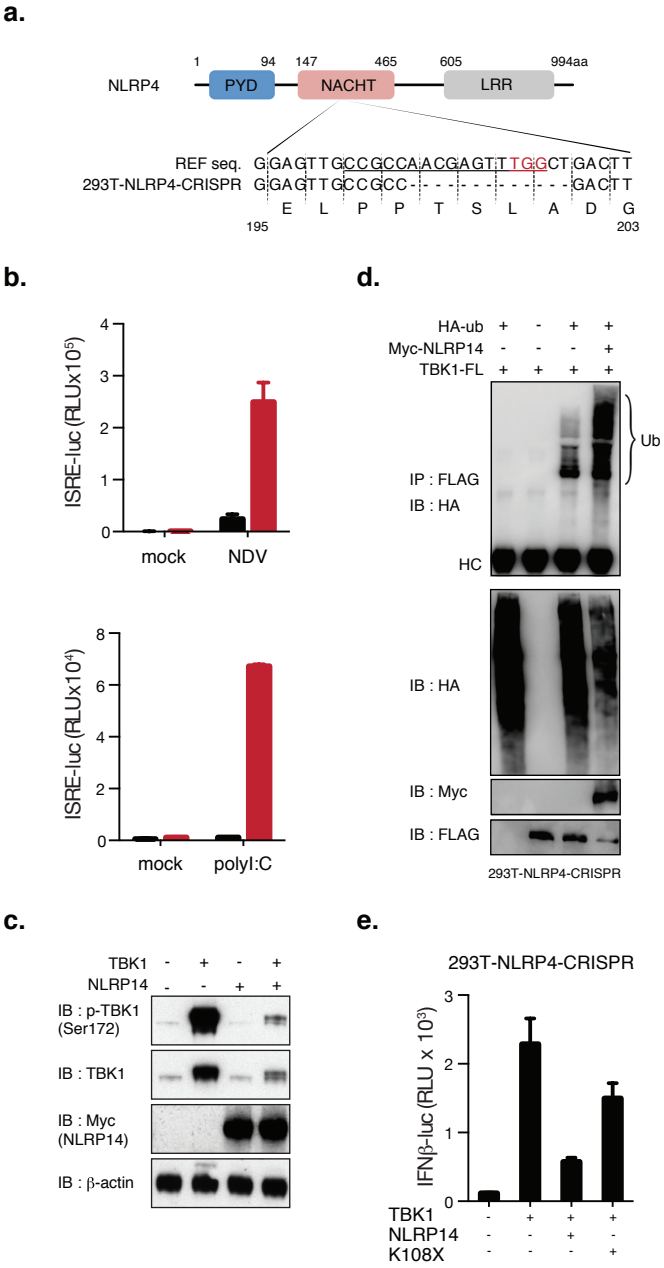
a.
NLRP4
1
94
147
465
605
994aa
PYD
NACHT
LRR
REF seq. GGAGTTGCCGCCACACGAGTTTGGCTGACTT
293T-NLRP4-CRISPR GGAGTTGCCGCC----------GACTT
E L P P T S L A D G
195
203
b.
ISRE-luc (RLUx10^5)
mock
NDV
ISRE-luc (RLUx10^4)
mock
polyI:C
c.
TBK1
NLRP14
IB : p-TBK1 (Ser172)
IB : TBK1
IB : Myc (NLRP14)
IB : β-actin
d.
HA-ub
Myc-NLRP14
TBK1-FL
Ub
IP : FLAG
IB : HA
HC
IB : HA
IB : Myc
IB : FLAG
293T-NLRP4-CRISPR
e.
293T-NLRP4-CRISPR
IFNβ-luc (RLU x 10^3)
TBK1
NLRP14
K108X

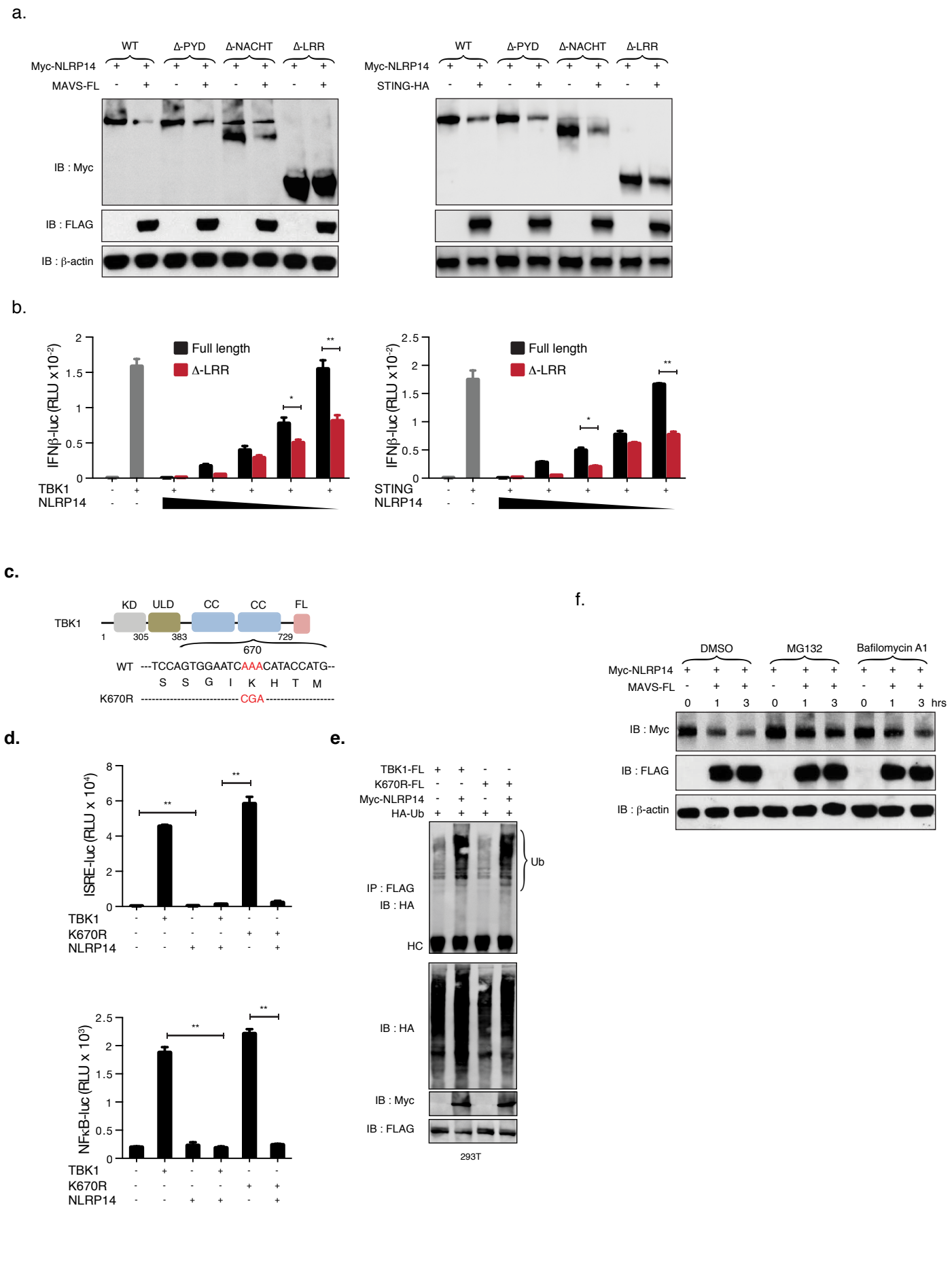
a.
WT
Δ-PYD
Δ-NACHT
Δ-LRR
Myc-NLRP14
MAVS-FL
STING-HA
IB : Myc
IB : FLAG
IB : β-actin
b.
Full length
Δ-LRR
IFNβ-luc (RLU x10-2)
TBK1
STING
NLRP14
c.
KD
ULD
CC
CC
FL
TBK1
1
305
383
729
670
WT ---TCCAGTGGAATCAAACATACCATG--
S S G I K H T M
K670R ---------- CGA ----------
d.
ISRE-luc (RLU x 10⁴)
NFκB-luc (RLU x 10³)
TBK1
K670R
NLRP14
e.
TBK1-FL
K670R-FL
Myc-NLRP14
HA-Ub
Ub
IP : FLAG
IB : HA
HC
IB : HA
IB : Myc
IB : FLAG
293T
f.
DMSO
MG132
Bafilomycin A1
Myc-NLRP14
MAVS-FL
0 1 3 0 1 3 0 1 3 hrs
IB : Myc
IB : FLAG
IB : β-actin

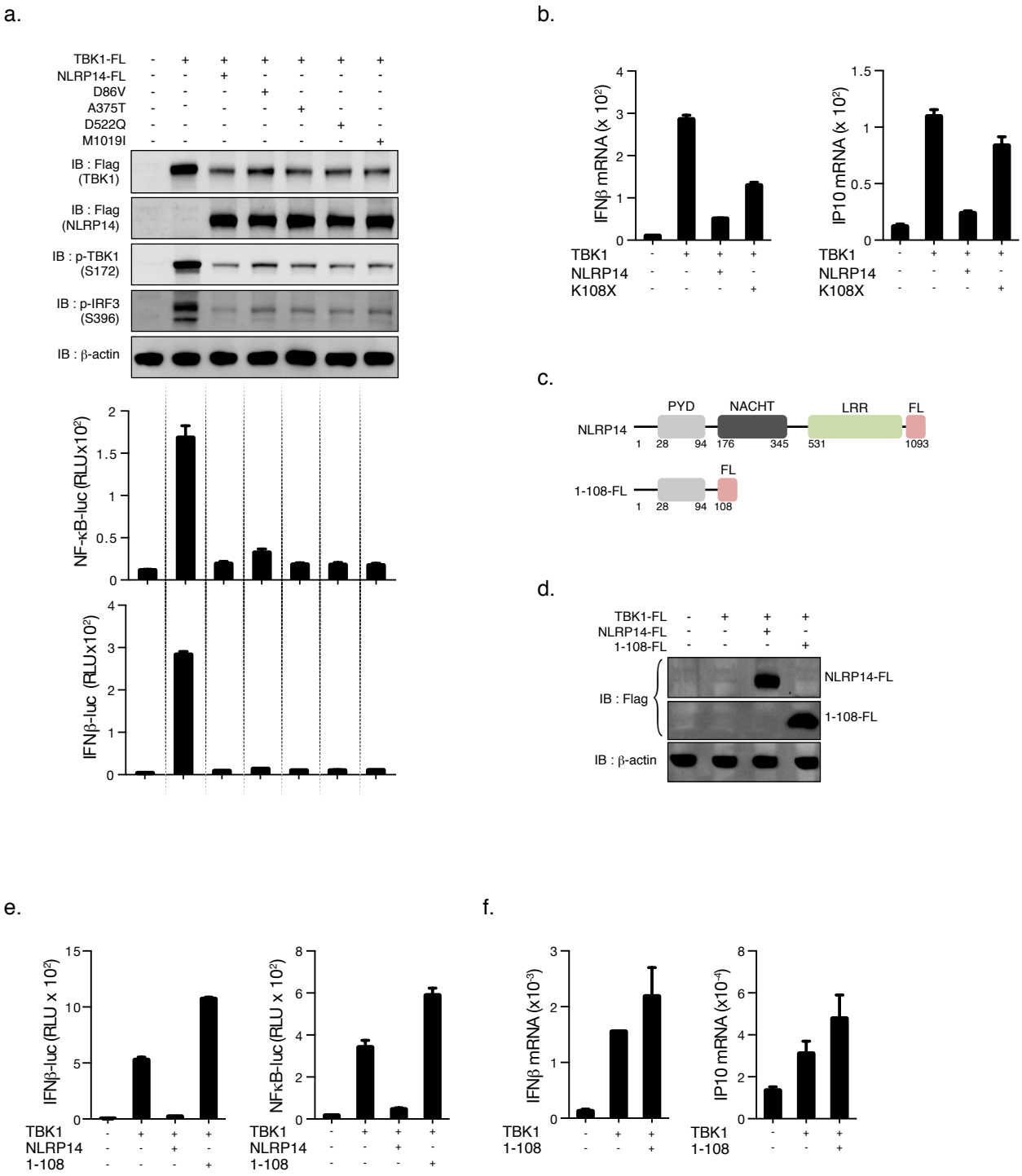
a.
TBK1-FL
NLRP14-FL
D86V
A375T
D522Q
M1019I
IB : Flag (TBK1)
IB : Flag (NLRP14)
IB : p-TBK1 (S172)
IB : p-IRF3 (S396)
IB : β-actin
NF-κB-luc (RLUx10²)
IFNβ-luc (RLUx10²)
b.
IFNβ mRNA (x 10²)
IP10 mRNA (x 10²)
TBK1
NLRP14
K108X
c.
NLRP14
PYD
NACHT
LRR
FL
1 28 94 176 345 531 1093
1-108-FL
1 28 94 108
d.
TBK1-FL
NLRP14-FL
1-108-FL
IB : Flag
IB : β-actin
e.
IFNβ-luc (RLU x 10²)
NFκB-luc (RLU x 10²)
TBK1
NLRP14
1-108
f.
IFNβ mRNA (x10⁻³)
IP10 mRNA (x10⁻⁴)
TBK1
1-108

Gene	RefSeq	EtrtrezID	SPR FPKM	Oo FPKM	1C FPKM
Ddx58	NM_172689	230073	3.49265	6.21611	13.7693
Tbk1	NM_019786	56480	15.068	5.75776	9.21457
Irf3	NM_016849,NR_045611	54131	10.3631	5.26195	1.5826
Mavs	NM_001206382,NM_001206383,NM_001206385,NM_144888	228607	10.0954	15.7585	16.8123
Traf3	NM_001286122,NM_011632	22031	3.79894	5.2888	10.7513
Traf6	NM_009424	22034	8.76028	0.897822	2.53922
Ifnar1	NM_010508	15975	9.8854	7.35525	7.25313
Mb21d1	NM_173386	214763	0.577828	23.1384	16.6859
Ddx41	NM_134059	72935	16.6363	17.5956	9.71526
Trex1	NM_001012236,NM_011637	22040	23.0882	1.3553	1.96993
Tmem173	NM_001289591,NM_001289592,NM_028261	72512	2.8505	0	0.0139251
Tlr3	NM_126166	142980	2.41825	2.14173	1.97696

Source: DBTMEE (Database of Transcriptome in Mouse Early Embryos)

References

1. Park SJ, Komata M, Inoue F, Yamada K, Nakai K, Ohsugi M, Shirahige K,
"Inferring the choreography of parental genomes during fertilization from ultralarge-scale whole-transcriptome analysis",
Genes Dev. 2013 Dec 15;27(24):2736-48

2. Brooke LaFlamme, "Gene expression in early development",
Nat Genet 46, 99 (2014)

Tissue	alias	number of samples
Esophagus	ES	227
Blood Vessel	BV	221
Brain	BRN	151
Skin	SK	146
Adipose Tissue	AT	135
Heart	HR	123
Muscle	MS	121
Lung	LN	120
Thyroid	TH	107
Nerve	NR	85
Stomach	ST	81
Colon	CL	74
Breast	BRS	65
Pancreas	PN	65
Testis	TS	60
Adrenal Gland	AG	52
Prostate	PR	42
Uterus	UT	36
Ovary	OV	35
Liver	LV	34
Spleen	SP	34
Vagina	VG	34
Pituitary	PT	22
Small Intestine	SI	17
Bladder	BL	11
Cervix Uteri	CU	9
Kidney	KD	8
Fallopian Tube	FT	6
Salivary Gland	SG	5